Nuclear Engineering and Technology 56 (2024) 2563–2569

Contents lists available at ScienceDirect

Nuclear Engineering and Technology

journal homepage: www.elsevier.com/locate/net

Original Article

Vibrational enhancement of evolutionary monochromatic neutron transport

Nassar H.S. Haidar

Euclidean Press LLC, 77 Ibrahim Abdul Al Str., Hamra, Beirut, Lebanon

ARTICLE INFO

Keywords:
Neutron density waves
Vibrational enhancement
Interference
Interface
Monochromatic neutron transport
Evolutionary
Rayleigh-like waves

ABSTRACT

The monochromatic hyperbolic neutron density wave is conceived as a Rayleigh-like wave with mixed transverse and longitudinal components. It is proved for the first time that the absolute ratio of the longitudinal to transverse interfering components, varies, with increasing the frequency of this wave, from zero to 1. Such a limited variation is to be coined as vibrational enhancement of evolutionary one-speed neutron transport.

1. Introduction

A great deal of literature, [1–7], exists in the field of nuclear science and technology on the propagation of neutron waves in nonmultiplying and/or multiplying media. The monochromatic model for dynamical neutronic fields is the simplest model from the analytical point of view, as energy-dependent waves are much harder to analyze. The closest setup to a monochromatic neutron field is a population of thermal neutrons of most probable neutron speed $\upsilon = 2200$ m/s. This population is assumed to exist in a medium with a Maxwellian neutron energy distribution over the 0–0.1 eV range, corresponding to an average neutron energy of 0.0253 eV, at 20 °C, with the Principle of Detailed Balance, [8,9], holding.

It is well known that transverse and longitudinal waves can be described by the same mathematical expressions, but to mean different "orthogonal" fluctuations. Seismic surface waves, [10], which travel slower than body waves are a mixture of both of these waves that exist on the same space–time $(x - t)$ domain. An example of this is the Rayleigh wave, [10], and its special form, called the Love wave.

The seismic Rayleigh wave, contemplated here is a wave that propagates along the surface of a semi-infinite elastic solid, and can still be conceived as a plane wave, [10,11]. It is a combination of longitudinal and transverse components that result from a 2D geometric spreading of a surface wave relative to a 3D geometric spreading of a body wave, [12]. The mechanical properties of the surface layer and body can be entirely different and the ratio of the longitudinal to transverse components is frequency-dependent. Seismic frequencies are, however, rather low as they are restricted to the range of 1–20 Hz. The Rayleigh-like model for the neutron density wave, resembles the seismic Rayleigh wave only in being a mixture of longitudinal and transverse waves in a ratio that distinctively depends on the singular spectrum of frequencies of the neutronic boundary vibration. The seismic and neutronic Rayleigh waves happen to differ in their source-geometry aspects. Consequently they are expected to differ, as well, in their wavefront, [13], configurations. Nevertheless, the existing literature on processing and applications of seismic Rayleigh waves is enormous, see e.g. [11,12,14], and references there in. It is hoped then that future analysis of the similar neutronic Rayleigh waves can benefit a good deal from this literature.

2. Analysis

The neutron wave $\phi(x,t)$ entertained in this work is conceived, as in the classical literature, [1–3,8,9], as a fluctuation around a steady state component $\Phi_s(x)$ of a neutron flux

$$\Phi(x,t) = \Phi_s(x) + \phi(x,t)$$

which could be of the same order of magnitude of $\Phi(x,t)$,i.e.

$$|\phi(x,t)| \leq \Phi(x,t).$$

Moreover, the parabolic 1-D monochromatic neutron wave, [1–3], $\phi(x,t)$,which is rederived in Appendix A, can be a finite, in $x \in \Re$ and $t \in [0,\infty)$, solution to a boundary-value problem (BVP), on a semi-infinite wedge, $\Re = [0,\infty)$, for the dynamical source-free neutron diffusion equation,

$$\frac{1}{\upsilon D}\nabla_t \phi + \frac{\Sigma_a}{D}\phi - \triangle_x \phi = 0\,, \tag{1}$$

subject to an oscillatory boundary $(x = 0)$ neutron current

$$I(0,t) = J(t) = \mathrm{Re}\left[\frac{J_0}{2}e^{i\ \omega t}\right], \tag{2}$$

E-mail address: nhaidar@suffolk.edu.

https://doi.org/10.1016/j.net.2024.02.015
Received 29 August 2022; Received in revised form 4 October 2023; Accepted 7 February 2024
Available online 8 April 2024

supplemented by an additional Fickian constitutive law,

$$I = -D\,\nabla_x\,\phi, \tag{3}$$

which relates the neutron flux ϕ to the neutron current.

Here $\frac{J_0}{2}$ and ω are respectively the amplitude and frequency of $I(0,t)$, while D is the diffusion coefficient and Σ_a is the neutron absorption macroscopic cross section for the wedge. $\mathfrak{R}$ is also assumed to be neutronically non-multiplying just for simplicity of the forthcoming analysis.

This remarkably happens despite the fact that the diffusion equation-being parabolic-cannot support oscillatory functions, [3,15], in its general solution. The neutron diffusion equation is, incidentally, only a rough approximation to neutron transport -a mathematically hyperbolic process - [15,16]. This approximation can be valid only at low frequencies, [5,17]. Moreover when the diffusion model is used, one tacitly concedes that the neutron wave propagates in the medium with infinite speed. However, since the amplitude of this wave decays exponentially fast in space, then this infinite speed paradox can be ignored in many applications, see, e.g. [18,19].

In distinction, the hyperbolic version of this $\phi(x,t)$ wave is a finite, in x and t, solution to a BVP for a P_1- approximation [4,5], to the neutron transport equation, which embeds a non-Fickian constitutive law, [6], subject to the same boundary current (2). This law is generalized-Fickian,

$$\xi\nabla_t I \; + \; I = -D\nabla_x\phi, \tag{4}$$

for a neutron current, I, fluctuation, and happens to be only one equation in a system of two coupled partial differential equations (PDEs) that form the P_1-canonical system, [7], of first-order PDEs. In (4) ξ is a temporal relaxation time,

$$\xi = \frac{3D}{\upsilon} \; = \frac{1}{\upsilon\Sigma_{tr}} \; , \tag{5}$$

in which υ is the speed of the monochromatic neutrons and Σ_{tr} is the macroscopic neutron transport cross-section, [7], of $\mathfrak{R}$.

Substitution of (4) in (1) transforms, [8,9], the previous canonical system to the equivalent second-order telegraphic PDE

$$\frac{3}{\upsilon^2}\triangle_t\phi + \frac{1}{\upsilon D}\left(1+\xi\;\upsilon\Sigma_a\right)\;\nabla_t\phi \;+\; \frac{\Sigma_a}{D}\phi - \;\triangle_x\phi = 0. \tag{6}$$

This PDE represents the P_1-approximation to dynamical neutron transport, and can be rewritten in the more compact form:

$$\frac{1}{\varsigma^2}\triangle_t\phi + a^2\;\nabla_t\phi \;+\; b^2\phi - \;\triangle_x\phi = 0, \tag{7}$$

where

$$a^2 \;=\; \frac{1}{\upsilon D}\left(1+\xi\;\upsilon\Sigma_a\right), \qquad b^2 = \;\frac{\Sigma_a}{D}\;\;, \qquad \frac{1}{\varsigma^2} = \frac{3}{\upsilon^2}, \tag{8}$$

with

$$\varsigma^2 \;=\; \frac{\upsilon D}{\xi}. \tag{9}$$

The associated BVP is also solved in Appendix A. Furthermore, the flux $\phi(x,t)$, of (7), for monochromatic neutrons can be scaled down by υ to define the neutron density wave (NDW)

$$N(x,t) = \phi(x,t)/\upsilon, \tag{10}$$

which travels with a phase speed, [3], $V_p \;=\; \sqrt{2\upsilon D\omega}$ and obeys the telegraphic P_1-approximation to the transport NDW

$$\frac{3}{\upsilon^2}\triangle_t N + \frac{1}{\upsilon D}\left(1+\xi\;\upsilon\Sigma_a\right)\;\nabla_t N \;+\; \frac{\Sigma_a}{D}N - \;\triangle_x N = 0. \tag{11}$$

Compared with the parabolic DE, (7) contains an additional second-order term $\frac{1}{\varsigma^2}\triangle_t\,\phi$, with "viscous damping" coefficient $\varsigma^2\;a^2$ and $\varsigma^2\;b^2$ "restoration" coefficient. All coefficients of are independent of ω, but may depend on ξ, Σ_a, υ and/or D. Moreover, according to (6), in the limit of $\xi\;\rightarrow\;0$, $\varsigma\;\rightarrow\;\infty$, and the entire reverts back to the parabolic equation.

When the macroscopic neutron absorption cross section Σ_a in $\mathfrak{R}$ is zero, the diffusional NDW becomes mathematically isomorphic with a temperature wave, [3], and both of them are transverse waves. Moreover, diffusional NDWs are known, [3,17–20] to propagate without neutron transfer. In contrast, NDWs in the context of neutron transport theory show similarities with plasma waves, [21], which are longitudinal. This is expected to facilitate their propagation with an accompanying neutron transfer.

Interestingly, the physical consistency of modeling the propagation of a neutron density wave by a Rayleigh-like wave should not be questionable. Indeed, in the absence of scattering : $\Sigma_{tr}\,=0$, i.e. when $D\rightarrow\infty$ (particularly when $\Sigma_a=0$), the incident neutron wave cannot be supported and cannot change direction of propagation; i.e. it would travel longitudinally. The earlier developed neutronic wave happens to predict this simple behavior in the limit of $\Sigma_{tr}\;=\;0$, or $D\;\rightarrow\;\infty$ when, according to (1), the transverse parabolic component can vanish at $x=0$.

The parabolic NDW, which travels with infinite speed, can be conceived as a special case of the hyperbolic NDW (which travels with a finite speed $\varsigma\;=\;\frac{\upsilon}{\sqrt{3}}$, [5]) when $\xi\;=\;0$. Let $\mathbf{x}$ and $\mathbf{y}$ be orthogonal unit vectors pointing in the $x>0$ and $y>0$ directions to phenomenologically accept that the hyperbolic NDW can define, $\triangleq$, a vector on the x–y plane viz

$$N(x,t)\triangleq\mathbf{Z}\;, \tag{12}$$

and

$$N_0(x,t)\triangleq Y(x,t)\mathbf{y}\;, \tag{13}$$

to accompany

$$N_1(x,t)\;\;\triangleq X(x,t)\mathbf{x}\;,$$

with $N_0(x,t)$ as a diffusional transverse, [3], component and $N_1(x,t)$ as a higher-order transport longitudinal component. It should be noted here that the notation "$\triangleq$" above means *defines* but not *equals*, and it is implicitly anticipated that only $N_1(x,t)$ can be accompanied by neutron transfer. Furthermore the neutrons of $N(x,t)$ can be conceived as a rarefied neutron gas to invoke, as constructively explained in Appendix B, Boyle's law

$$P(x,t)\frac{1}{X(x,\,t)}\sim RT\;,$$

in which $X(x,t)$ in [n/cm^3] is a neutron density fluctuation similar to $Y(x,t)$ but orthogonal to it, R is the universal gas constant, [9], and T is the absolute temperature of the neutron gas. The Appendix ends in (B.10) with

$$X(x,t) = \;CP(x,t),$$

proportional to a fluctuation in the pressure, in [atm], of the neutron gas, and

$$C = 4.1\times10^{19}\text{n/atm cm}^3,$$

emerges as a virial-like constant. Then we are motivated enough to hypothesize for $N(x,t)$ a vectorial additive decomposition principle that follows.

Principle 1. *The hyperbolic NDW is a Rayleigh-type wave, i.e. it is decomposable viz*

$$\mathbf{Z} = X\mathbf{x}\; + Y\mathbf{y} = X(x,t)\mathbf{x} + Y(x,t)\mathbf{y}, \tag{14}$$

where

$$|\mathbf{Z}|^2 = |X\mathbf{x}|^2\;\; + |Y\mathbf{y}|^2,$$

or equivalently

$$N^2(x,t) = {N_1}^2(x,t) + {N_0}^2(x,t) \tag{15}$$

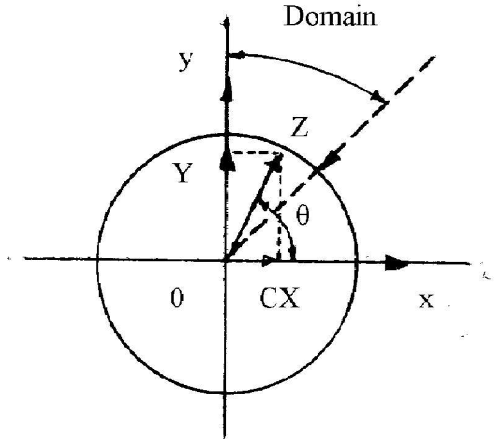

Fig. 1. Sketch to illustrate the components of the neutron wave at a fixed time moment.

Proof. By consistency of the results obtained in (30) and (45) with (14)–(15).

The phenomenological principle above is an effective replacement of the sum of a transverse, $N_0(x,t)$, and longitudinal, $N_1(x,t)$, components by an equivalent sum of two orthogonal transverse components, $Y(x,t)$ **y** and $C\ X(x,t)$ **x**, as illustrated by Fig. 1, which may consistently interfere. Clearly, the transverse $N_0(x,t) \triangleq Y(x,t)$ **y** wave fluctuates vertically on x, while the longitudinal $N_1(x,t) \triangleq X(x,t)$ **x** wave fluctuates parallel to x. Moreover, according to Rayleigh-wave seismic terminology, if $\eta\ (x,t) = \frac{N\ (x,t)}{N_0(x,t)} = csec\ \theta$, then the ratio

$$\beta(x,t) = \frac{N_1(x,t)}{N_0(x,t)} = \sqrt{[\eta^2(x,t) - 1]} = ctan\theta, \tag{16}$$

may be conceived as "ellipticity", [12,22], of $N(x,t)$. Incidentally $\beta \lesssim \eta$ and the Love wave is a special case of the Rayleigh-wave when the associated $\|\beta\| \to \infty$.

The solution in Appendix A for the hyperbolic BVP can be shown, [17], to infer the existence of a critical frequency $\omega_c = 2\pi\ f_c = \frac{2\pi}{\xi}$, at which the neutron wave phase speed $V_p = \sqrt{2\upsilon D\ \omega}$ becomes a ω–independent $\varsigma = \sqrt{\frac{\upsilon D}{\xi}}$. This is similar to the situation with temperature waves, [17,20], where $\omega_c = \frac{2\pi}{\gamma}$, and γ is the temperature relaxation time. The basic difference between the two waves stems from the different scales for their ξ and γ.Indeed $\gamma \ll \xi$, as γ is pico-scaled, while ξ is micro-scaled. Moreover, since for a temperature wave, with diffusivity α, the $V_p = \sqrt{2\alpha\ \omega}$ transforms, as of $f_c = \frac{1}{\gamma} \sim 10^{12}$ Hz, [17,20], to $u = \sqrt{\frac{\alpha}{\gamma}} \sim 10^3$ m/s, which is of the same order of magnitude of sound speed in solids. This is one of the reasons why u was, historically, called the second sound speed, [22], which can be sensed only when $f > f_c \sim 10^{12}$ Hz. As for neutron density waves, since the speed of sound in D_2O, e.g., is 1480 m/s, [9], and $D = 8.1 \times 10^{-3}$ m, then $\xi = \frac{\upsilon D}{\varsigma^2} = 11.1 \times 10^{-6} = 11.1$ μs.Correspondingly, $f_c = \frac{1}{\xi} = 9 \times 10^4$ Hz $= 90\ k$ Hz. Furthermore, $\varsigma = \sqrt{\frac{\upsilon D}{\xi}} = \frac{\upsilon}{\sqrt{3}} = 1270$ m/s is a constant for all media, which is less than the speed of sound that exceeds 1480 m/s. Clearly then there is no need for a concept like "second neutron wave speed" similar to the second sound speed, [22].

It should be noted here that experimental data on both ξ and γ is difficult to obtain due to difficulties in measurements of both ς and u and in generating the required f 's. For instance, with the exception of liquid Helium, no reliable experimental data has so far been reported, [23–25], for γ. Also, there appears to be a shortage of experimental data on ξ,as well. Nevertheless, non-Fourier effects have recently been observed in a variety of phenomena involving ultra fast heating such as supernovae explosions, [26], or laser power pulsations [27]. There is no reason why this subject cannot possibly extend, in a different setting, to cover also non-Fickian effects in neutron transport.

The rest of this note shall investigate the impact of this principle on $\beta\ (x,t)$ and its possible implications.

3. Ellipticity of hyperbolic neutron density waves

Let us look at the ratio $\eta\ (x,t) = \frac{N\ (x,t)}{N_0(x,t)}$, of (A.14) to (A.15), as a function of ω, throughout the wedge, in general, and at its $x = 0$ boundary, in particular. This ratio is representable as

$$\eta(x,t) = \rho(\omega)E(x;\omega)W(x,t;\omega) \tag{17}$$

where

$$\rho(\omega) = \frac{A^2 + B^2}{\widetilde{A}^2 + \widetilde{B}^2} = \sqrt{\frac{\omega^2 + \upsilon^2\ \Sigma_a{}^2}{(1+\xi\ \upsilon\ \Sigma_a)^2\ \omega^2 + (\xi\ \omega^2 - \upsilon\Sigma_a)^2}}, \tag{18}$$

$$E(x;\omega) = e^{(A-\widetilde{A})\ x}, \tag{19}$$

$$W(x,t;\omega) = \frac{(\xi\omega\widetilde{B} + \widetilde{A})\ cos(\widetilde{B}\ x - \omega t) + (\xi\omega\widetilde{A} - \widetilde{B}\ )\ sin\left(\widetilde{B}\ x - \omega t\ \right)}{(\xi\omega B + A)\ cos\ (Bx - \omega t) + (\xi\omega A - B)\ sin\,(Bx - \omega t\ )}. \tag{20}$$

In view of the dependence of A, B, $\widetilde{A}$ and $\widetilde{B}$ on the set $\{\upsilon, D, \Sigma_a, \xi, \omega\}$, $\eta\ (x,t)$ can tractably be analyzed only at the extreme ends of the ω spectrum.

3.1. Low frequency ellipticity

Below the critical frequency $\omega_c = \frac{2\pi}{\xi}$, i.e. when $0 \le \xi\ \omega \ll 1$, it can, by inspection, be demonstrated that

$$\begin{pmatrix} A \\ B \end{pmatrix} \approx \left(\begin{array}{c} \sqrt{\frac{\Sigma_a}{D}} \\ \frac{\omega}{2\upsilon\ \sqrt{D\Sigma_a}} \end{array} \right), \tag{21}$$

$$\begin{pmatrix} \widetilde{A} \\ \widetilde{B} \end{pmatrix} \approx \left(\begin{array}{c} \sqrt{\frac{\Sigma_a}{D}}\left[1 - \frac{\xi\ \omega^2}{2\ \upsilon\ \Sigma_a}\right] \\ \frac{(1\ +\ \xi\ \upsilon\Sigma_a)\ \omega}{2\upsilon\ \sqrt{D\Sigma_a}} \end{array} \right), \tag{22}$$

$$\rho(\omega) \approx 1 \Big/ \sqrt{\frac{(1+\xi\ \upsilon\ \Sigma_a)^2\ \omega^2}{\omega^2 + \upsilon^2\ \Sigma_a{}^2} + \frac{(\xi\ \omega^2 - \upsilon\Sigma_a)^2}{\omega^2 + \upsilon^2\ \Sigma_a{}^2}},$$

when $\omega \ll \upsilon\ \Sigma_a$,while $\upsilon\ \xi\ \Sigma_a \ll 1$ (which is true for all neutron moderators), satisfies

$$\rho(\omega) \approx \frac{1}{\sqrt{\xi^{\ 2}\omega^2 + 1}}. \tag{23}$$

The small term $\xi\ \upsilon\Sigma_a\ \omega$ is retained in (22) because of the possibility for high enough values of $\upsilon\Sigma_a$. Also the small term $\xi^{\ 2}\omega^2$ is retained in (23) to allow for values of $\xi\ \omega$ closer to 1. Then

$$E(x;\omega) \approx e^{\frac{1}{2}\frac{\xi\ \omega^2}{\upsilon\ \sqrt{D\ \Sigma_a}}\ x} \approx 1, \tag{24}$$

$$W(x,t;\omega) \approx \frac{\sqrt{\frac{\Sigma_a}{D}}\ cos(\widetilde{B}\ x - \omega t) - \frac{(1\ +\ \xi\ \upsilon\ \Sigma_a)\ \omega}{2\ \upsilon\ \sqrt{D\Sigma_a}}\ sin\left(\widetilde{B}\ x - \omega t\ \right)}{\sqrt{\frac{\Sigma_a}{D}}\ cos\ (Bx - \omega t) - \frac{(1\ +\ \xi\ \upsilon\ \Sigma_a)\ \omega}{2\ \upsilon\ \sqrt{D\Sigma_a}}\ sin\,(Bx - \omega t\ )}. \tag{25}$$

Therefore $W(x,t;\omega)$ is expressible viz,

$$W(x,t;\omega) \approx \cos\omega\left(\frac{(1 + \xi\ \upsilon\ \Sigma_a)}{2\ \upsilon\ \sqrt{D\Sigma_a}}\ x - t\right)\ \sec\omega\left(\frac{1}{2\ \upsilon\ \sqrt{D\Sigma_a}}\ x - t\right), \tag{26}$$

which is the same as

$$W(x,t;\omega) \approx \left[1 - \tan\frac{\xi}{2}\sqrt{\frac{\Sigma_a}{D}}\ \omega x\ \tan\omega\left(\frac{1}{2\ \upsilon\ \sqrt{D\Sigma_a}}\ x - t\right)\right]$$

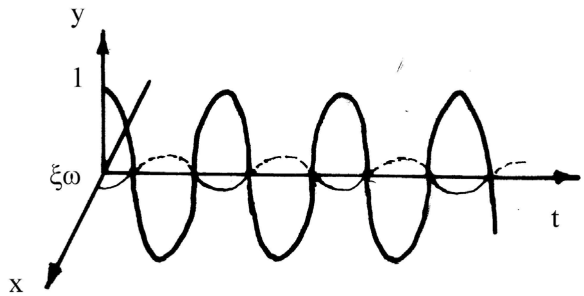

Fig. 2. Sketch to illustrate the Y and X components of the interfacial low frequency ($\xi\omega \ll 1$) neutron density wave.

$$\times \cos \frac{\xi}{2} \sqrt{\frac{\Sigma_a}{D}}\, \omega x. \tag{27}$$

It is remarkable how the $x = 0$ interface happens to be the simplest spatial point, for a neutron density wave, with regard to analysis of ellipticity. Indeed,

$$E(0;\omega) = W(0,t;\omega) \;= 1, \;\; \eta(0,t) = \frac{1}{\sqrt{\xi^{\,2}\omega^2 + 1}}, \tag{28}$$

and

$$\beta(0,t) = \frac{N_1(0,t)}{N_0(0,t)} = \sqrt{[\eta^2(0,t) - 1]} = \sqrt{\frac{1}{\xi^{\,2}\omega^2 + 1} - 1} \;=\; \xi\omega i\,. \tag{29}$$

Hence when $\xi\,\omega \ll 1$ the longitudinal component $N_1(0,t) \triangleq X(x,t)$ **x** of the interfacial NDW is only a tiny fraction of the transversal component $N_0(x,t) \triangleq Y(x,t)$ **y**, with a $\frac{\pi}{2}$ phase shift, viz,

$$X(0,t)\mathbf{x} \approx \xi\omega i\; Y(0,t)\mathbf{y},$$

or

$$N_1(0,t) = \mathrm{Im}\left[\, e^{i\frac{\pi}{2}}\;\xi\omega N_0(0,t)\right]\,, \tag{30}$$

which is an assertion of orthogonality of the actions of $N_1(0,t)$ and $N_0(0,t)$. *The consistency of this result with (14) serves as a proof of the correctness of the underlying Principle 1*.

Moreover, it can then, by inspection, be verified that

$$N_0(x,t) = \frac{1}{\upsilon\sqrt{D\Sigma_a}}\;\frac{J_0}{2}\;\; e^{-\sqrt{\frac{\Sigma_a}{D}}\,x} \cos\omega\left(\frac{1}{2\,\upsilon\sqrt{D\Sigma_a}}\;x - t\right)\,, \tag{31}$$

$$N(x,t) = \frac{1}{\upsilon\sqrt{D\Sigma_a}}\;\frac{J_0}{2}\;\frac{1}{\sqrt{\xi^{\,2}\omega^2+1}}\;\; e^{-\sqrt{\frac{\Sigma_a}{D}}\,x}$$
$$\times \cos\omega\left(\frac{(1+\xi\,\upsilon\,\Sigma_a)}{2\,\upsilon\sqrt{D\Sigma_a}}\;x - t\right). \tag{32}$$

The last three relations demonstrate that, for low ω, and at the at $x = 0$ boundary, the NDW and its two components are

$$N(0,t) = \frac{1}{\upsilon\sqrt{D\Sigma_a}}\;\frac{1}{\sqrt{\xi^{\,2}\omega^2+1}}\;\frac{J_0}{2}\;\cos\omega t, \tag{33}$$

$$N_0(0,t) = \frac{1}{\upsilon\sqrt{D\Sigma_a}}\;\;\frac{J_0}{2}\;\cos\omega t, \tag{34}$$

$$N_1(0,t) = \mathrm{Im}\left[\, e^{i\frac{\pi}{2}}\;\xi\omega\,\frac{1}{\upsilon\sqrt{D\Sigma_a}}\;\;\frac{J_0}{2}\;\cos\omega t\right], \tag{35}$$

and that they satisfy (15) via $N^2(0,t) = N_0^2(0,t) + N_1^2(0,t)$, when $\xi\,\omega \ll 1$. The interference between $N_1(0,t) \triangleq X(0,t)$ **x** and $N_0(0,t) \triangleq Y(0,t)$ **y**, noted above, is clearly ω-dependent, as demonstrated in Fig. 2.

It should be underlined, however, that in the limit of $\omega = 0$, $N_1(0,t)$ should always vanish. This can be physically incorrect, in reflection to the approximate nature of the present analysis.

3.2. High frequency ellipticity

At high frequencies, i.e. when $\xi\,\omega \gg 1$, the situation happens to be entirely different. Above the critical frequency ω_c, V_p transforms to ς. Here

$$\begin{pmatrix} A \\ B \end{pmatrix} \approx \begin{bmatrix} \frac{1}{\mu}\left(1 + \frac{\Sigma_a}{\omega}\right) \\ \frac{1}{\mu}\left(1 - \frac{\Sigma_a}{\omega}\right) \end{bmatrix}, \tag{36}$$

$$\begin{pmatrix} \widetilde{A} \\ \widetilde{B} \end{pmatrix} \approx \begin{pmatrix} \frac{(1\,-\,\xi\;\upsilon\Sigma_a)}{2\sqrt{\upsilon\;D\;\xi}} \\ \frac{\omega}{\varsigma} \end{pmatrix}, \tag{37}$$

$$\rho(\omega)\;\approx\;\frac{1}{\sqrt{\xi^{\,2}\omega^2 + \;(1+\xi^2\;\upsilon^2\;\Sigma_a^2)}}\;\approx\;\frac{1}{\xi\;\omega} \tag{38}$$

$$E(x;\omega)\;\approx e^{\frac{1}{\mu}\left[1\,+\,\left(\frac{1}{2\;\omega}\;+\sqrt{\frac{\xi}{2}}\;\frac{\upsilon}{\sqrt{\omega}}\right)\Sigma_a\;-\frac{1}{\sqrt{2\;\xi\omega}}\right]\;x}, \tag{39}$$

and

$$W(x,t;\omega)\;\;\approx\;\;\frac{\frac{\xi}{\varsigma}\;\omega^2\;cos(\widetilde{B}\;x-\omega t)\;-\;\frac{(1\,+\,\xi\;\Sigma_a)}{2}\;\frac{\omega}{\varsigma}\;sin\left(\widetilde{B}\;x-\omega t\;\right)}{\frac{1}{\mu}(\xi\;\omega+1)\;\;cos\;(Bx-\omega t)+\frac{1}{\mu}(\xi\;\omega-1)\;\;sin\,(Bx-\omega t\;)}. \tag{40}$$

Therefore $W(x,t;\omega)$ can be approximated viz

$$W(x,t;\omega)\;\;\approx \mu\frac{\omega}{\xi}\;\frac{cos(\widetilde{B}\;x-\omega t)}{cos\;(Bx-\omega t)+sin\,(Bx-\omega t\;)}$$
$$= \mu\frac{\omega}{\sqrt{2}\;\xi}\;\frac{cos(\widetilde{B}\;x-\omega t)}{cos\;(Bx-\omega t\;-\frac{\pi}{4})}. \tag{41}$$

For $\xi\,\omega \gg 1$, one can ignore $\frac{\pi}{4}$ in the denominator of (25) to rewrite it as

$$W(x,t;\omega)\;\;\approx \mu\frac{\omega}{\sqrt{2}\;\xi}\;\frac{cos(\frac{\omega}{\varsigma}x-\omega t)}{cos\left[\frac{1}{\mu}\left(1-\frac{\Sigma_a}{\omega}\right)x-\omega t\right]}. \tag{42}$$

$$W(0,t;\omega)\;\;= \mu\frac{\omega}{\sqrt{2}\;\xi}\;\;= \sqrt{\,\xi\;\omega}\;\;\&\;\;\;\eta(0,t)\;\;=\;\frac{1}{\sqrt{\xi\omega}}. \tag{43}$$

It is remarkable how $\beta\;(0,t)$, when $\xi\,\omega \gg 1$, is just

$$\beta(0,t) = \sqrt{[\eta^2(0,t)-1]} = \sqrt{\frac{1}{\xi\;\omega} - 1}. \tag{44}$$

Since $\lim\limits_{\xi\omega \gg 1} \beta\;(0,t) = i$, then as $\xi\,\omega \gg 1$, $N_1(0,t) \triangleq X(0,t)$ **x** of the interfacial NDW becomes identical to $N_0(x,t) \triangleq Y(0,t)$ **y**,but for a $\frac{\pi}{2}$ phase shift, viz,

$$X(0,t)\mathbf{x} \approx i\;Y(0,t)\mathbf{y},$$

or

$$N_1(0,t) = \mathrm{Im}\left[\, e^{i\frac{\pi}{2}}\,N_0(0,t)\right], \tag{45}$$

which is another assertion of orthogonality of the actions of $N_1(0,t)$ and $N_0(0,t)$. *The consistency of this result with (14) serves as a further proof of the correctness of the underlying Principle 1*.

Furthermore, as in (31)–(32), it can be shown that

$$N_0(x,t) = \frac{\sqrt{\xi\omega}}{\varsigma}\;\frac{J_0}{2}\;\;e^{-\frac{1}{\mu}\,x}\cos\omega\left(\frac{1}{\mu}\;x-t\right), \tag{46}$$

$$N(x,t) = \frac{1}{\varsigma}\;\frac{J_0}{2}\;\;e^{-\frac{1}{\mu}\left(1\,+\,\frac{\Sigma_a}{\omega}\right)\,x}\cos\omega\left(\frac{1}{\varsigma}\;x-t\right). \tag{47}$$

Relations lead directly to

$$N(0,t) = \;\;\frac{1}{\varsigma}\;\frac{J_0}{2}\;\;\cos\omega t\;, \tag{48}$$

$$N_0(0,t) = \;\;\frac{\sqrt{\,\xi\omega}}{\varsigma}\;\frac{J_0}{2}\;\;\cos\omega t\;, \tag{49}$$

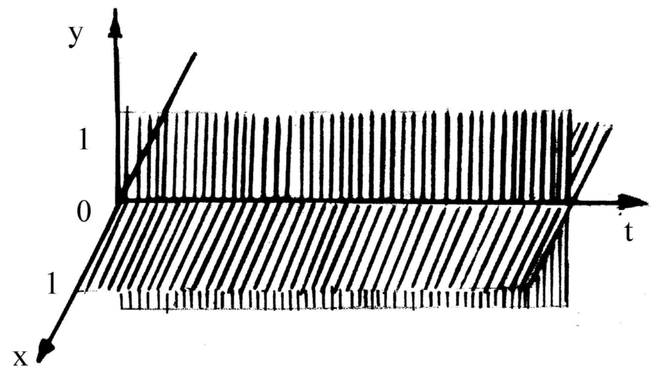

Fig. 3. Sketch to illustrate the Y and X components of the interfacial high frequency ($\xi\omega \gg 1$) neutron density wave.

$$N_1(0,t) \;=\; \mathrm{Im}\left[e^{i\frac{\pi}{2}} \frac{\sqrt{\xi\omega}}{\varsigma} \frac{J_0}{2} \cos\omega t \right] . \tag{50}$$

that are illustrated in Fig. 3. The plot in this figure indicates that the domain for Z, mentioned in Fig. 1, should subtend an angle of $\frac{\pi}{4}$.

These relations infer a distinctive nearly ω-free semi-diagonal interference between $N_1(0,t) \triangleq X(0,t)$ **x** and $N_0(0,t) \triangleq Y(0,t)$ **y** and satisfy, when $\xi\ \omega \gg 1$, $N^2(0,t) = N_0^2(0,t) + N_1^2(0,t)$.

4. Neutron transport enhancement by vibration

Since ellipticity of hyperbolic NDWs varies dramatically with varying ω, it should be interesting to identify the frequency ω_* at which the transition occurs between the previous two different modes of behavior of $\beta\ (0,t)$. This can follow from uniqueness of the magnitude of $N(0,t)$, $\forall t$,by relations (33) and (50), viz

$$\frac{1}{\upsilon\ \sqrt{D\Sigma_a}} \quad \frac{1}{\sqrt{\xi^{\ 2}\omega^2+1}} = \frac{1}{\varsigma} . \tag{51}$$

The solution ω_* of this algebraic equation is

$$\omega_* = \frac{1}{\xi}\sqrt{\frac{1}{\upsilon\ \xi\ \Sigma_a} - 1} ,$$

where $\upsilon\ \xi\ \Sigma_a \ll 1$, for all neutron moderators, to become

$$\omega_* \approx \frac{1}{\xi\ \sqrt{\upsilon\Sigma_a\ \xi}} \gtrsim \omega_c = \frac{2\pi}{\xi} , \tag{52}$$

which happens to be of the order of 10^8 rad/s for graphite, [6,9], and of 10^7 rad/s for D_2O. Hence the low-ω and high-ω domains for $\beta\ (0,t)$ are $\Lambda = \{\omega : 0 < \omega < \omega_*\}$ and $\Gamma = \{\omega : \omega_* \le \omega < \infty\}$,respectively.

Consequently,

$$\left|N_1(0,t)\right| \begin{cases} \ll \left|N_0(0,t)\right| , & \omega \in \Lambda \\ = \ \ \left|N_0(0,t)\right| , & \omega \in \Gamma \end{cases} , \tag{53}$$

where the transverse wave $N_0(0,t)$ travels with nonrelativistic infinite speed, while the longitudinal wave $N_1(0,t)$ travels with a finite speed $\varsigma = \frac{\upsilon}{\sqrt{3}} = \sqrt{\frac{\upsilon D}{\xi}}$.This demonstrates that the NDW $N(0,t)$ is a Rayleigh-like wave with an absolute ellipticity that cannot exceed unity by increasing ω. Furthermore, since longitudinal NDW propagation is accompanied by neutron transfer, then enhancement of evolutionary neutron transport, by increasing the wave frequency, is constrained by (53). These results are certainly generalizable, from the interface $x = 0$ to any $x \in \mathfrak{R}$, after a due consideration of the strong exponential spatial decay of $N(x,t)$.

5. Discussion

In the preceding sections, the mixed transverse-longitudinal nature of a hyperbolic (P_{-1} transport) NDW is analyzed, for the first time, in the framework of a Rayleigh wave model. A frequency-dependent interfacial ellipticity $\beta\ (0,t)$ is established in (29) and (44) to vary restrictively on (0,1), by varying ω over $(0,\infty)$.The frequency singular domain is shown by (53) to be characteristically divisible into two subdomains, at a discrete transition frequency ω_* of (54).

Although the underlying principle (14)–(15) for the Rayleigh wave model is only phenomenological, i.e. not foundational or microscopic, it is proved, nevertheless, to be mathematically consistent. Physically, however, it may not be sharp enough, but can certainly be expected to hold at least in some approximate fashion. Any future sharpening of our findings on $\beta(0,t)$ calls for a preceding experimental verification of them, at least for some technically feasible frequencies. Such experimental measurements of $\beta(0,t)$,as a function of ω,using accelerator-based modulated neutronic beams, [18], may not be simple and can even be rather costly.

6. Conclusion

We have demonstrated in this work that the frequency of a hyperbolic vibrating neutron population is a defining factor for the transport/diffusion ratio content (ellipticity) of its NDW. This justifies the claim for a vibrational enhancement of neutron transport. The Rayleigh wave model is shown to lead to mathematically consistent and physically verifiable results for the interfacial ellipticity of a NDW. The reported analysis is developed along the steps that follow.

(i) Introduction of the telegraphic P_{-1} transport (hyperbolic) NDW in Section 2. Here also a phenomenological principle is advanced to support a Rayleigh wave model for the NDW.

(ii) A review of the analytical solution, in Appendix A, to the BVP's for both parabolic and hyperbolic NDW's.

(iii) Definition, in Section 3, of ellipticity for a NDW and a study of its approximate behavior at low and high vibrational frequencies.

(iv) Establishment, in Section 4, that vibrational frequency can restrictively enhance the ellipticity of a NDW.

Generalization of the reported interfacial results to points deep inside the NDW supporting wedge $\mathfrak{R}$,remains, however, a pending mathematical question.

In fairness to similar research on heat transfer, one needs to mention that Cattaneo–Vernotte type BVPs, similar to (11) + (2) + (4), can admit solutions with specific resonances, [28]. On another note, frequency optimization of the NDW $N(x,t)$ has recently found particular applications in dynamical neutron cancer therapy, [18,19]. The validity of Principle 1, which calls for experimental verification, is expected, moreover, to widen the horizons for this optimization. The present frequency-enhancement of evolutionary neutron transport is, however, entirely different from heat transfer enhancement by surface vibration, reported in [29], for example. It even has nothing to do with it.

Declaration of competing interest

The authors declare that they have no known competing financial interests or personal relationships that could have appeared to influence the work reported in this paper.

Data availability

Data can be derived from public domain resources.

Acknowledgments

The author is grateful to the anonymous referees for a number of valuable suggestions and comments on an earlier version of this paper.

Appendix A. Parabolic and hyperbolic neutron density waves

A.1. Parabolic neutron density waves

A separated variables finite solution, $N(x,t) = X(x)\, e^{i\,\omega t}/\,\upsilon$, to (1), when subjected to satisfaction of (2)–(3), with

$$\mu = \mu(\omega; D) = \sqrt{\frac{2\upsilon D}{\omega}} \quad and \quad \varepsilon = \sqrt{\frac{D}{\upsilon}}\ , \tag{A.1}$$

leads, see e.g. [7,15,16], to the conventional parabolic NDW,

$$N(x,t) = \left(J_0 \,/[2\upsilon D\,(A^2 + B^2)]\right) e^{-A\,x} \times [A\,cos\,(Bx-\omega t) - B\,sin(Bx-\omega t\,)], \tag{A.2}$$

where

$$\left\{\begin{array}{c} A \\ B \end{array}\right\} = \sqrt{\frac{\Sigma_a}{2\,D}}\sqrt{\sqrt{\frac{\omega^2}{\upsilon^2\,\Sigma_a{}^2}+1} \pm 1} = \frac{1}{\sqrt{2\,\upsilon\,D}}\sqrt{\sqrt{\omega^2+\upsilon^2\,\Sigma_a{}^2} \pm \upsilon\,\Sigma_a}\,. \tag{A.3}$$

For any set $\{\omega, D, \Sigma_a\}$, when $\Sigma_a \neq 0$,it is obvious that $A > B \approx \frac{1}{\mu}$, and relation (A.2) can, using the identity

$$A\cos\gamma - B\sin\gamma = \mathfrak{A}\,\cos(\gamma-\theta)\ ;\ \mathfrak{A} = \sqrt{A^2+B^2}\ ;\ \theta = -\tan^{-1}\frac{B}{A}\ ,\ \forall\,\gamma,$$

be demonstrated to be always convertible to

$$N(x,t) = \left(J_0 \,/[2\upsilon D\,\sqrt{A^2+B^2}\,]\right) e^{-A\,x}\,cos\left(Bx-\omega t+\tan^{-1}\frac{B}{A}\right), \tag{A.4}$$

where,

$$\frac{B}{A} = \sqrt{\frac{\sqrt{\frac{\omega^2}{\upsilon^2\,\Sigma_a{}^2}+1} - 1}{\sqrt{\frac{\omega^2}{\upsilon^2\,\Sigma_a{}^2}+1} + 1}}\ , \tag{A.5}$$

happens to be independent of D.

Important special cases of (A.2) are the following

(i) If $\Sigma_a = 0$,then $A = B = \frac{1}{\mu}$ and

$$N(x,t) = \frac{J_0}{2\upsilon\,\varepsilon\sqrt{\omega}}\, e^{-\frac{x}{\mu}}\,cos\left(\frac{x}{\mu} - \omega t + \frac{\pi}{4}\right). \tag{A.6}$$

(ii) If $\omega \ll \upsilon\Sigma_a$, then $A = \sqrt{\frac{\Sigma_a}{D}}$, $B = 0$ and (A.2) becomes

$$N(x,t) = \frac{J_0}{2\upsilon\sqrt{D\Sigma_a}}\, e^{-\sqrt{\frac{\Sigma_a}{D}}\,x}\,cos\omega t\,. \tag{A.7}$$

(iii) Conversely, If $\omega \gg \upsilon\Sigma_a$, then $A = B \to 0$ and

$$N(x,t) \equiv 0\,. \tag{A.8}$$

This result is a clear reflection of the inconsistency of the neutron diffusion model for the NDW at very high ω.

A.2. Hyperbolic neutron density waves

$\phi(x,t)$ is obtained here, as in [17,20], also via separation of variables: $\phi(x,t) = Y(x)\,e^{i\,\omega t}$.In application to (7), this leads to the Helmholtz equation

$$Y'' - æ^2 Y = 0,$$

with

$$æ = \sqrt{a^2\omega\, i - \left(\frac{\omega^2}{\varsigma^2} - b^2\right)} = \pm(\widetilde{A} + i\widetilde{B}), \tag{A.9}$$

where

$$\left\{\begin{array}{c} \widetilde{A} \\ \widetilde{B} \end{array}\right\} = \sqrt{\frac{1}{2}\left(\sqrt{\left(\frac{\omega^2}{\varsigma^2} - b^2\right)^2 + a^4\omega^2} \mp \left(\frac{\omega^2}{\varsigma^2} - b^2\right)\right)}, \tag{A.10}$$

which is the same as

$$\left\{\begin{array}{c} \widetilde{A} \\ \widetilde{B} \end{array}\right\} = \sqrt{\frac{\xi\,\omega^2 - \upsilon\Sigma_a}{2\upsilon D}\left(\sqrt{\left(\frac{(1+\xi\,\upsilon\Sigma_a)\,\omega}{\xi\,\omega^2 - \upsilon\Sigma_a}\right)^2 + 1} \mp 1\right)}. \tag{A.11}$$

It is straight forward to demonstrate that $\left\{\begin{array}{c} \widetilde{A} \\ \widetilde{B} \end{array}\right\}$ tends to $\left\{\begin{array}{c} A \\ B \end{array}\right\}$ tends to $\xi = 0.$ of (A.3) when $\phi(x,t)$

Finiteness of $\phi(x,t), \forall,\ x$ & t, allows for writing

$$\phi(x,t) = \ Ce^{-\widetilde{A}\,x}\, e^{-i\left(\widetilde{B}\,x - \omega t\right)}\,.$$

Then to determine the C constant, the non-Fickian BC (4) :

$$\xi\nabla_t I(x,t)\,|_{x=0} + I(x,t)\,|_{x=0} = -D\nabla_x\phi(x,t)\,|_{x=0}, \tag{A.12}$$

is invoked, when $I(x,t)\,|_{x=0} = I(0,t) = J(t)$ of (1.2). As a result,

$$C = \left(J_0 \,/[2D\,(\widetilde{A}^2 + \widetilde{B}^2)]\right)\left[(\xi\omega\widetilde{B} + \widetilde{A}) + i\,(\xi\omega\widetilde{A} - \widetilde{B}\,)\right].$$

Consequently, the hyperbolic NW is

$$\phi(x,t) = \left(J_0 \,/[2D\,(\widetilde{A}^2 + \widetilde{B}^2)]\right) e^{-\widetilde{A}\,x}\left[(\xi\omega\widetilde{B} + \widetilde{A})\,cos(\widetilde{B}\,x - \omega t) + (\xi\omega\widetilde{A} - \widetilde{B}\,)\,sin\left(\widetilde{B}\,x - \omega t\right)\right], \tag{A.13}$$

and the associated hyperbolic NDW is $\xi = 0$,

$$N(x,t) = \left(J_0 \,/[2\upsilon D\,(\widetilde{A}^2 + \widetilde{B}^2)]\right) e^{-\widetilde{A}\,x}\left[(\xi\omega\widetilde{B} + \widetilde{A})\,cos(\widetilde{B}\,x - \omega t) + (\xi\omega\widetilde{A} - \widetilde{B}\,)\,sin\left(\widetilde{B}\,x - \omega t\right)\right]. \tag{A.14}$$

It is straightforward to verify that when $\xi = 0$ relation is the same as (A.2), i.e., ϕ,

$$N_0(x,t) = \left(J_0 \,/[2\upsilon D\,(A^2 + B^2)]\right) e^{-A\,x} \times [A\,cos\,(Bx-\omega t) - B\,sin(Bx-\omega t\,)]\,. \tag{A.15}$$

Appendix B. Neutrons as an ideal gas in nuclear reactors

It is well known, [8,9], that neutrons in nuclear reactors, even with high fluxes, ϕ, of the order of $10^{13} - 10^{15}$ n/cm^2 s, behave like a rarefied ideal gas, i.e. with pressures on below the nano atmosphere scale.

To estimate the magnitude of pressures associated with such fluxes, we shall reasonably assume neutrons to constitute a single species in their gas then to invoke Boyle's law

$$PV = \nu RT, \tag{B.1}$$

in which P is pressure in [atm], V is the molar volume in [l], T is temperature in [°K], R is the universal gas constant

$$R = 0.082057 \text{ atm l /mole. °K}, \tag{B.2}$$

and ν is the molar number in [mole]. In this respect, for an H_2 gas $\upsilon = 2$ moles, whereas for D^+ ions, (p+n), $\nu = 1$ mole. We may artificially expand the concept of υ to cover nuclear particles to assume for this D^+ that $\upsilon = 2$ that "moles". Extension of this approach to neutrons means for them a $\upsilon = 1$ "mole". It should be noted however that this extension is foundationally incorrect and hence should be avoided in any practical evaluation based on (B.1), as we shall see later in this appendix.

Furthermore, the ratio

$$\frac{PV}{\nu RT} = 1,$$

is called the compression factor, which is a measure of the ideality of any gas. The greater this ratio deviates from 1, the more it will behave like a real gas.

For a neutron density wave $X = \frac{1}{V} = X(x,t)$ the unit is [n/cm^3], and this can be related to (B.1) via the gas mechanical density

$$\sigma = \frac{m}{V} = mX, \tag{B.3}$$

where m is the mass in [g] and satisfies

$$m = M\nu,$$

with M being a molar mass in [g/mole], which is 1 g/mole for neutrons. Therefore (B.1)

$$\sigma = \frac{M\ \nu}{V} = M\nu X \quad \text{and} \quad \frac{\sigma}{M} = \frac{\nu}{V} = \nu X\ . \tag{B.4}$$

Rewrite then (B.1) as

$$\nu X = \frac{P}{RT}\ , \tag{B.5}$$

to combine (B.4) and (B.5) in the form

$$\sigma = \frac{PM}{RT}\ , \tag{B.6}$$

which is explicitly independent of the undesirable ν.

Since σ is in [g/l] and the neutron mass is

$$m_o = 1.674663 \times 10^{-24}\text{g}\ , \tag{B.7}$$

then

$$X = \frac{MP}{\nu MRT} = \frac{M\ P}{m_o RT}\ [n/l] = .\ \frac{M\ P}{10^3\ m_o RT}\ [\text{n/cm}^3] \tag{B.8}$$

Substitute then $M = 1$ with (B.2) and (B.7), when $T = 20\,°C = 293\,°K$ in (B.8) to obtain

$$X = CP = 4.1 \times 10^{19} P\ , \tag{B.9}$$

in n/cm^3, when P is in atm. Conversely,

$$P = 2.44 \times 10^{-20} X = C^{-1} X \tag{B.10}$$

where C can be conceived only as a phenomenological empirical constant.

Assume further that, at standard temperature and pressure, the thermal neutron average speed υ in a neutron gas to be 2200 m/s. Hence

$$X = \frac{\phi}{2.44\ \times\ 10^5} = 4.545 \times 10^{-6}\phi. \tag{B.11}$$

As for neutron fluxes in common nuclear reactors, i.e. $\phi \approx 10^{13}$ n/cm^2.s, the neutron densities, according to (B.11), are $X \approx 4.545 \times 10^7$, n/cm^3. Ultimately, relation (B.9) provides an empirical estimate for the neutron gas associated pressure

$$P = 1.11 \times 10^{-12}\ \text{atm} = \ \ 1.11\ \text{p atm},$$

which is clearly on the pico atmosphere scale.

References

[1] R.B. Perez, R.E. Uhring, Propagation of neutron waves in moderating media, Nucl. Sci. Eng. 17 (1) (1963) 90–100.
[2] M.J. Ohanian, R.S. Booth, R.B. Perez, Eigenfunction analysis of neutron-wave propagation in moderating media, Nucl. Sci. Eng. 30 (1) (1967) 75–103.
[3] N.H.S. Haidar, Neutron density waves versus temperature waves, Int. J. Adv. Nucl. React. Des. Technol. 3 (2021) 206–212.
[4] G.F. Niderauer, Neutron Kinetics Based on the Equation of Telegraphy (Ph.D. Dissertation), Iowa State University, US, 1967.
[5] H. Hayasaka, S. Takeda, Study of neutron wave propagation, J. Nucl. Sci. Technol. 5 (11) (1968) 564–571.
[6] H. Gomez, I. Colominas, F. Navarrina, J. Paris, M. Casteleiro, A hyperbolic theory for advection-diffusion problems: Mathematical foundations and numerical modeling, Arch. Comput. Meth. Eng. 11 (2010) 191–211.
[7] G.I. Bell, S. Glasstone, Nuclear Reactor Theory, Van Nostrand, New York, US, 1970.
[8] H. Soodak (Ed.), Reactor Handbook, III, A, Interscience, New York, US, 1962.
[9] K.H. Bekurts, K. Wirtz, Neutron Physics, Springer Verlag, Berlin, 1964.
[10] A. Berbellini, A. Moelli, A.M.G. Ferreira, Ellipticity of Rayleigh waves in basin and hard-rock sites in northern Italy, Geophys. J. Inter. 206 (1) (2016) 395–407.
[11] I.A. Viktoro, Rayleigh and Lamb Waves: Physical Theory & Applications, Plenum Press, New York, US, 1967.
[12] S. Ooi, Rayleigh Wave Interactions with Tribological Contacts, (Ph.D. thesis), University of Sheffield, UK, 2015.
[13] N.H.S. Haidar, On physical and mathematical wave fronts in temperature waves, Transylv. J. Math. Mech. 14 (2) (2022) 139–158.
[14] L. Mandel, Color imagery by wavefront reconstruction, J. Opt. Soc. Amer. 55 (12) (1965) 1697–1698.
[15] L. Herrera, D. Pavón, Hyperbolic theories of dissipation: Why and when we need them ? Physica A : Stat. Mech. Appl. 307 (1–2) (2002) 121–130.
[16] A.M. Weinberg, E.P. Wigner, The Physical Theory of Neutron Chain Reactors, University of Chicago Press, Chicago, US, 1958.
[17] A. Salazar, Energy propagation of thermal waves, Eur. J. Phys. 27 (2006) 1349–1355.
[18] N.H.S. Haidar, A resonated and synchrophased three beams neutron cancer therapy installation, J. Nucl. Eng. Rad. Sci. 6 (2020) 034501.
[19] N.H.S. Haidar, Optimization of two opposing neutron beams parameters in dynamical (B/Gd) neutron cancer therapy, Nucl. Energy Technol. 5 (1) (2019) 1–7.
[20] D.D. Joseph, L. Preziosi, Heat waves, Rev. Modern Phys. 61 (1) (1989) 41–73.
[21] T. Hinno, Y. Ozawa, Comparison between longitudinal wave in electron plasma and one-velocity neutron transport, J. Nucl. Sci. Technol. 12 (2) (1975) 107–114.
[22] H. Beck, P.F. Meier, A. Thellung, Phonon hydrodynamics in solids, Phys. Status Solid 24 (1974) 11–63.
[23] A. Graßmann, F. Peters, Experimental investigation of heat conduction in wet sand, Heat Mass Transf. 35 (1999) 289–294.
[24] W. Roetzel, N. Putra, S.K. Das, Experiment and analysis for non-Fourier conduction in materials with non-homogeneous inner structure, Int. J. Therm. Sci. 42 (2003) 541–552.
[25] J. Ordonez-Miranda, J.J. Alvarado-Gil, Thermal wave oscillations and thermal relaxation time determination in a hyperbolic heat transport model, Int. J. Therm. Sci. 48 (11) (2009) 2053–2062.
[26] N. Falcon, J. Labrador, Thermal waves and unstable convection in ZZ Ceti stars, Odessa Asrtronom. Public. 14 (2001) 141–143.
[27] J.K. Chen, D.Y. Tzou, J.E. Beraun, A semiclassical two-temperature model for ultrafast laser heating, Int. J. Heat Mass Transf. 49 (2006) 307–316.
[28] M. Xu, L. Wang, Thermal oscillations and resonance in dual-phase lagging heat conduction, Int. J. Heat Mass Transfer 45 (5) (2002) 1055–1061.
[29] A. Sathyabhama, S.P. Prashanth, Enhancement of boiling heat transfer using surface vibrations, Heat Transf.-Asian Res. 46 (1) (2015) 49–60.

Further reading

[1] P.G. Malischewsky, F. Scherbaum, Love's formula and H/V-ratio (ellipticity) of Rayleigh waves, Wave Motion 40 (1) (2004) 57–67.